

# A Sparkle-Rendering Model Based on Metrological Parameters

Aurora Larrosa<sup>1</sup>, Julián Espinosa<sup>1</sup>, Alejandro Ferrero<sup>2</sup>, Nina Basic<sup>3</sup>, Néstor Tejedor<sup>1</sup> and Esther Perales<sup>1</sup>.

<sup>1</sup>Departamento de Óptica, Farmacología y Anatomía, Universidad de Alicante, Alicante, Spain.

<sup>2</sup>Instituto de Óptica, Consejo Superior de Investigaciones Científicas (CSIC), Madrid, Spain.

<sup>3</sup>Eidgenössisches Institut für Metrologie (METAS), Bern-Wabern, Switzerland

## Abstract

E-commerce has become the primary global shopping method, but the inability to physically inspect products presents challenges for consumers. This study focuses on the sparkle texture effect, significant in various industries. Evaluation tools are limited to two instruments, leading the International Commission on Illumination (CIE) to work on establishing measurement scales, like such applied in [1]. The study proposes a rendering model sparkle utilising a metrologic scale based on the luminous point density and visibility probability distribution, by assuming a half-Gaussian shape which should be fitted to measurement data in order to obtain parameters  $\mu$  and  $\sigma$ . The model algorithm was computed for 25 samples across three different geometries (15°:0°, 45°:0° and 75°:0°). The maximum deviation between measurements and the fitted function was found to be 0.09, indicating negligible discrepancies in terms of cumulative probability. The analysis revealed that  $\mu$  tends to approach zero for all samples, while  $\sigma$  showed a correlation with the density of sparkle points  $d_s$ , with a Pearson correlation coefficient exceeding 0.91 for all geometries, indicating a strong relationship between the two variables. A preliminary rendering is obtained, using Mobile Display Characterisation and Illumination Model (MDCIM) for the background colour.

## Introduction

In recent years, especially after the COVID-19 pandemic, e-commerce has become the primary worldwide shopping method. Despite its ease and convenience, this evolving commercial model presents a significant disadvantage for consumers: they are unable to physically inspect the products they intend to buy and must rely solely on the visual appearance displayed on their screens. The term *appearance* refers to the visual sensation through which attributes of an object are perceived [2]. The visual appearance of a material is characterised by four perceptual attributes: colour, gloss, texture, and translucency.

This proceeding will focus on the texture effect known as *sparkle*. This phenomenon might be observed in the automotive industry, as well as in other industrial sectors such as printing, plastics, cosmetics, textiles, etc. The use of special-effect pigments is a common practice in these industries. These pigments induce a significant colour shift depending on the angles of illumination and observation. Beyond this angular colour dependency, materials incorporating special-effect pigments are perceived by humans with textures referred to as *sparkle* and *graininess* [3]. Specifically, *sparkle* is defined as the presence of small bright points against a significantly darker background under directional lighting, meaning that this points will have visibility ( $V$ ) greater than 0. On the other hand, *graininess* is characterised by an irregular light-to-dark pattern observed under conditions of diffuse lighting.

Despite the characterisation and rendering of these two effects being crucial for the previously mentioned industries, there

are only two instruments designed for evaluating *sparkle* and *graininess*: the BYK-mac i multi-angle spectrophotometer by BYK-Gardner [4] and the MAT12 multi-angle spectrophotometer by X-Rite [5]. However, each instrument provides distinct parameters associated with both visual textures, and their results are not comparable. Consequently, the International Commission on Illumination (CIE) is actively involved in the development of measurement scales for these two texture effects [6]. In the context of this study, significant efforts have been devoted in recent years towards proposing a measurement scale correlated with visual perception [1]. This scale characterises *sparkle* by considering the density of luminous points and the probability distribution of their visibilities, details of which will be discussed in detail in subsequent sections of this work.

The development of a reproducible and reliable method for assessing the visual appearance of materials containing special-effect pigments is essential for the industries involved, aimed at enhancing product quality control. Additionally, achieving a realistic rendering of the visual appearance of products coated with these pigments is crucial for artificial visualisation in online sales scenarios. Consequently, the primary goal of this work is to propose a rendering model for special-effect coating samples based on the measurement scale for *sparkle* defined in [1].

## Methods

### Sample set and metrological parameters

In this study, a set of 25 samples from the Effect Navigator collection, manufactured by Standox [7], was employed. This set was previously utilised in [1] and [8]. These samples were manufactured with aluminium pigments, which will be called *flakes* [10], and black absorption pigments. Each sample is assigned an L number and an EN number, both ranging from one to five (see Figure 1). The L number correlates with the concentration of effect pigments, while the EN number increases with the greater average size of pigments in the sample and, consequently, a more pronounced *sparkle* effect as well [1].

In [1], the methodology employed for measuring *sparkle* in these samples is explained. Different goniophotometers were utilised to facilitate a comparison of the parameters delineated in the same article. These parameters are defined as follows:

- **Sparkle density** ( $d_s$ ). Number of points per square millimetre that are visible ( $V > 0$ ).
- **First visibility quartile** ( $V_{Q_1}$ ). Visibility threshold at which 25% of the remaining values are lower.
- **Second visibility quartile** ( $V_{Q_2}$ ). Visibility threshold at which 50% of the remaining values are lower.
- **Third visibility quartile** ( $V_{Q_3}$ ). Visibility threshold at which 75% of the remaining values are lower.

In order to obtain their metrological parameters, measurements of the 25 samples were conducted at three measurement geometries aligning with those found in commercially available

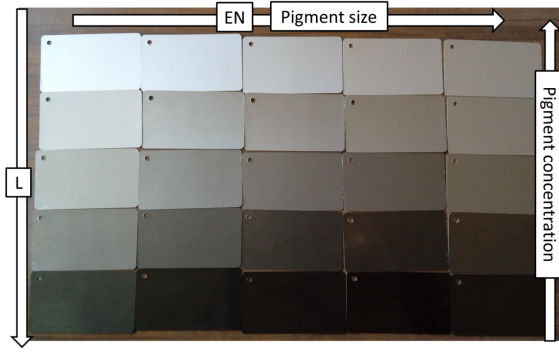


**Figure 1.** Standex special-effect pigment samples from the Effect Navigator collection.

instruments: 15°:0°, 45°:0° and 75°:0°. For this purpose, the measurements obtained from METAS will be employed [1].

### Sparkle-generation algorithm

As previously stated, the objective of this study is to propose a model for reproducing the characteristics of the *sparkle* points distribution in a special-effect coating sample on a digital display, utilising the metrological parameters from [1]. The model will be assessed using data acquired from samples within the Effect Navigator collection, measured at 15°, 45°, and 75° angles.

The visual perception of *sparkle* is defined by the presence of small starry points against the background. Only a subset of these points stands out significantly compared to others, which, although distinguishable from the background, do not exhibit the same level of notability. In this manner, *sparkle* can be explained by distinguishing between the background and the luminous points. When a background point within the sample is surrounded by other background points, its visibility  $V$  will be 0, whereas a *sparkle* point stands out from the background and thus possesses a visibility greater than 0. Consequently, it is expected that *sparkle* could be characterised by a probability distribution function of the visibilities of the *sparkle* points, separating them from the background (which will always have  $V = 0$ ). The orientation of the sparkles and distribution of size of pigments make rare the larger visibilities. Taking this into consideration and that prior rendering models [10] have postulated a Gaussian probability distribution for the orientation of *flakes* in special-effect pigments, this model proposes a Probability Distribution Function for the visibility of *sparkle* points (PDF( $V$ ), equation 1) drawn in accordance with a half-Gaussian-shaped curve.

$$\text{PDF}(V) = \begin{cases} 0 & V \leq \mu \\ \frac{2}{\sigma\sqrt{2\pi}} e^{-\frac{1}{2}\left(\frac{V-\mu}{\sigma}\right)^2} & V > \mu \end{cases} \quad (1)$$

In the previous expression,  $\mu$  represents the mean of the hypothesised complete Gaussian, while  $\sigma$  denotes its standard deviation. The objective would be to characterise the PDF curve with these parameters,  $\mu$  and  $\sigma$  through a fitting process to a set of known data. However, the available data comprises quartile values, not values explicitly belonging to PDF.

The Cumulative Distribution Function (CDF) for a given value  $V$  (equation 2) is defined as the integral of the Probability Distribution Function over the interval from negative infinity to the specified value:

$$\text{CDF}(V) = \int_{-\infty}^V \text{PDF}(x) dx \quad (2)$$

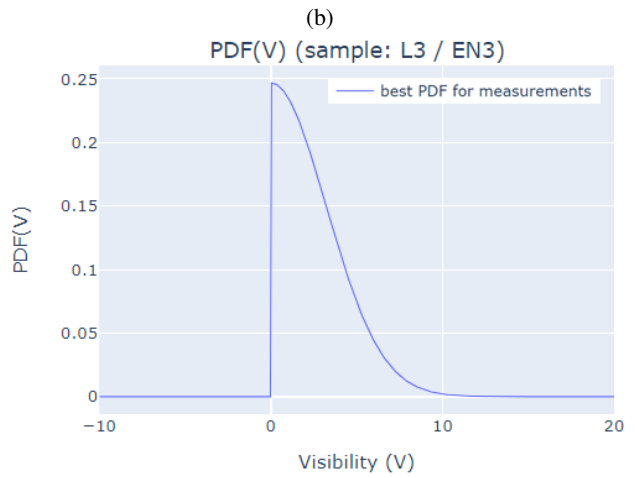
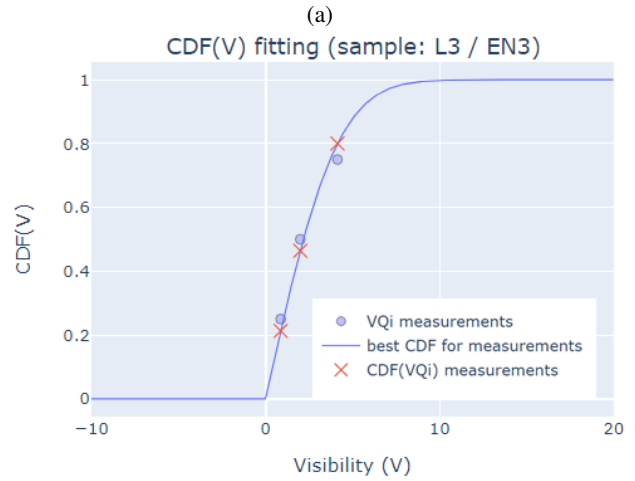


**Figure 2.** Visibility CDF for sample L3/EN3 at the 45°:0° geometry (a) and the corresponding PDF (b).

We know the quartiles of the distribution, and, by virtue of their inherent definition, we also possess the corresponding cumulative probability:  $\text{CDF}(V_{Q_1}) = 0.25$ ,  $\text{CDF}(V_{Q_2}) = 0.50$  and  $\text{CDF}(V_{Q_3}) = 0.75$ . Consequently, we have three pairs of coordinates  $(x_1, y_1) = (V_{Q_1}, 0.25)$ ,  $(x_2, y_2) = (V_{Q_2}, 0.50)$ ,  $(x_3, y_3) = (V_{Q_3}, 0.75)$  for which a fitting procedure can be employed to determine  $\mu$  and  $\sigma$  considering  $y = \text{CDF}(x)$ . The analytical expression for the Cumulative Distribution Function can be obtained by substituting (1) into (2). The resulting equation is presented as follows:

$$\text{CDF}(V) = \begin{cases} 0 & V \leq \mu \\ \text{erf}\left(\frac{V-\mu}{\sigma\sqrt{2}}\right) & V > \mu \end{cases} \quad (3)$$

Once the parameters  $\mu$  and  $\sigma$  are determined, it becomes feasible to generate an image with the corresponding number of *sparkle* points, considering the image dimensions and the *sparkle* points density  $d_s$ . Thus, a conversion of its units from points per square mm to points per pixel is necessary. This conversion requires knowledge of the screen's DPI (Dots Per Inch) parameter, where the *sparkle* is intended to be rendered. The visibility of the *sparkle* points will be randomly assigned based on the appropriate PDF corresponding  $\mu$  and  $\sigma$ .

This algorithm was conducted for the measurements of 25 samples within the sample set, covering each of the three distinct geometries.

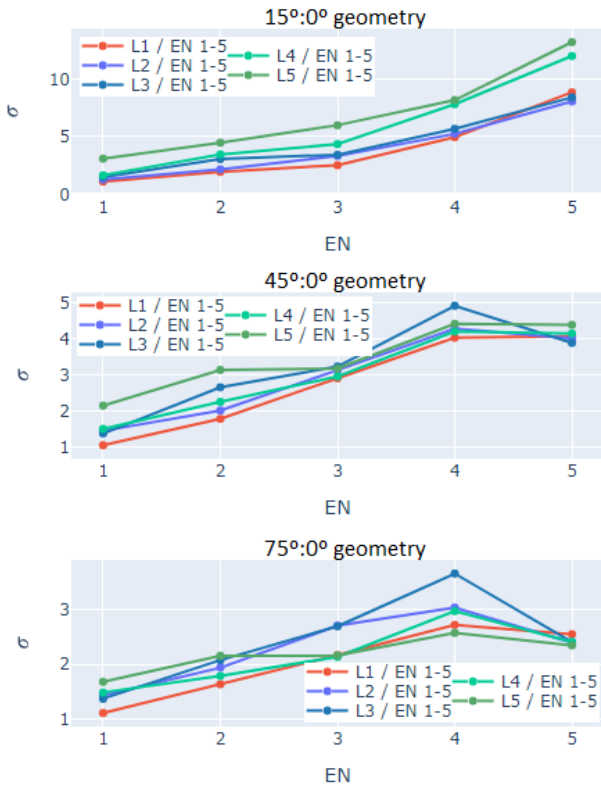


**Figure 3.** Parameter  $\sigma$  as a function of EN for each of the three measured geometries. The  $\sigma$  parameter varies with EN across the three measured geometries. Each trace depicts a subset of 5 samples with the same L, as indicated in the legend, while EN ranges from 1 to 5. Across all graphs, there is a noticeable upward trend in  $\sigma$  as EN (average pigment size).

## Results and discussion

The parameters  $\mu$  and  $\sigma$  were computed for the 25 samples shown in Figure 1 at geometries  $15^\circ:0^\circ$ ,  $45^\circ:0^\circ$  and  $75^\circ:0^\circ$ . The uncertainty estimation of the visibility CDF fitting was derived by determining the maximum absolute difference for the three data points between the assumed probability of the visibility quartiles and their corresponding values in the actual CDF. This maximum difference was found to be 0.09 for a total of 3 measurements, with all remaining discrepancies falling below this threshold. Given that these differences are in terms of cumulative probability, they are considered to be very low.

From the results of the parameters characterising the probability distribution, interesting insights can be derived. The parameter  $\mu$  is nearly zero for all samples, indicating that the probability of visible *sparkle* points is larger the lower is the visibility (maximum probability when V tends to zero). This is in line with expectations, given that negative visibility is nonsensical. On the other hand,  $\sigma$  ranges from 1.05 to 13.24 across the measurements. A higher  $\sigma$  corresponds to a broader half-Gaussian distribution and, consequently, an increased likelihood of obtaining points with elevated visibility during rendering. Figure 2 shows an example of the CDF and PDF for sample L3 / EN3 at the  $45^\circ:0^\circ$  geometry. In Figure 2 (a), the plot depicts the visibility CDF for this sample at the  $45^\circ:0^\circ$  geometry, along with the quartiles of the experimental measurements and their corresponding values on the CDF, as well as the PDF obtained with calculated  $\mu$  and  $\sigma$  in Figure 2 (b).

It is noteworthy to explore the potential association between  $\sigma$  and the structural characteristics of the samples or other parameters of the metrological model. In Figure 3, it can be ob-

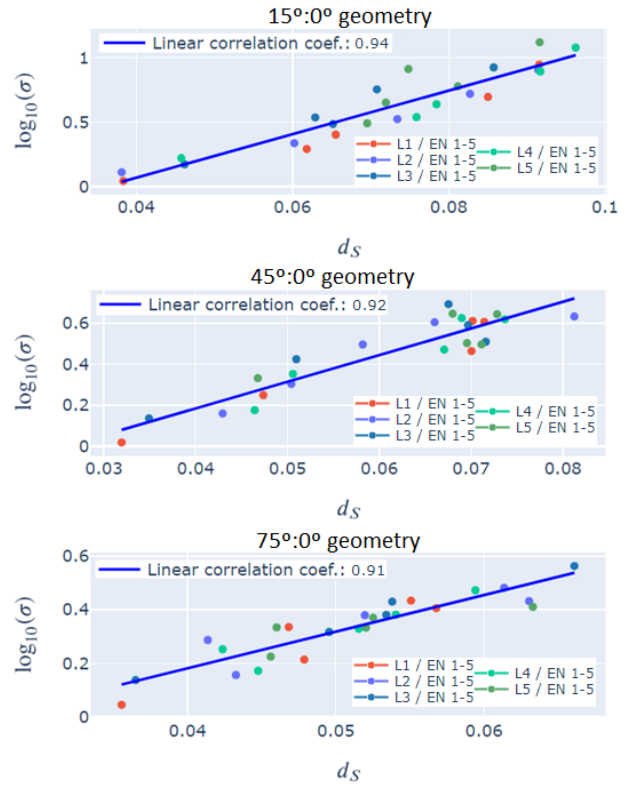


**Figure 4.** Logarithm of  $\sigma$  as a function of  $d_S$  for each of the three measured geometries. The logarithm of  $\sigma$  changes with the density of sparkle points  $d_S$  across the three measured geometries. Each set of dots of the same colour represents a subset of 5 samples with the same L, as shown in the legend, while EN ranges from 1 to 5. Across all graphs, there is a discernible correlation between both variables, indicating a tendency to increase together.

served that for each series of samples denoted with the same L,  $\sigma$  increases as EN also increases across all geometries. For  $15^\circ:0^\circ$ , this trend occurs up to EN5 in all series, whereas for  $45^\circ:0^\circ$  and  $75^\circ:0^\circ$ , this correlation persists up to EN4, beyond which it plateaus or, in some cases, even declines. This implies that  $\sigma$  increases with the size of the *flakes*. In other words, when a sample contains larger reflective pigments, there is a higher probability of perceiving bright points with high visibility. This will be observed in the rendering.

Additionally,  $\sigma$  demonstrates to be related to the density of *sparkle* points  $d_S$ . Similar to what happened with  $V_{Q_2}$  in [1],  $\sigma$  increases with  $d_S$ , although not linearly. Given the heteroscedasticity of the samples, a linear regression analysis between  $d_S$  and the logarithm of  $\sigma$  is performed, obtaining a Pearson correlation coefficient greater than 0.91 for all three geometries (Figure 4). This correlation suggests that when rendering, an increase in the number of *sparkle* points should correspond to a higher maximum visibility of the brightest point.

After calculating the parameters  $\mu$  and  $\sigma$ , a distribution of random points required for rendering was generated based on the PDF of each sample and in each geometry. As an initial exploration, the background colour and the colour of the *sparkle* points were depicted according to the laboratory lighting conditions using the MDCIM model [11, 12], which has exhibited robust colour reproduction in prior investigations. The preliminary outcome at  $45^\circ:0^\circ$  for sample L3/EN3 is depicted in Figure 5. And a comparison of samples with L (rows) and EN (columns) both 1, 3, and 5 in Figure 6.

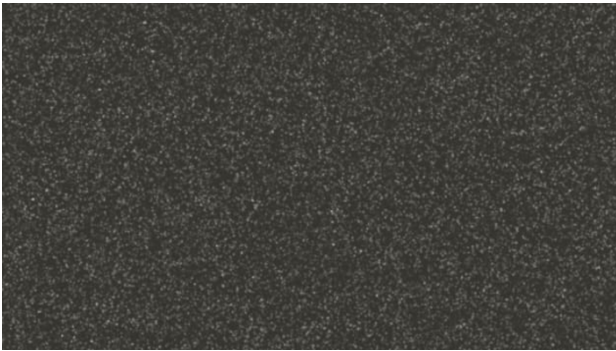


Figure 5. Preliminary rendering example for sample L3 / EN3 at 45°:0°.

## Conclusions

In this conference proceeding, we present the algorithm for calculating rendering parameters  $\mu$  and  $\sigma$  from  $V_{Q_1}$ ,  $V_{Q_2}$  and  $V_{Q_3}$ . The *sparkle* points density  $d_S$  is also required for rendering purposes. It has been observed that the  $\sigma$  parameter correlates positively with pigment size, as indicated by the EN parameter in the Effect Navigator samples (see Figure 3), and that its logarithm exhibits a linear relationship with the density of *sparkle* points (see Figure 4).

The current challenge lies in achieving, once the points are randomly generated according to their respective probability distributions, an appropriate gradient ranging from the background colour to the brightest *sparkle* points that closely resembles what the human eye could perceive. This task must consider effects such as the Point Spread Function, among others.

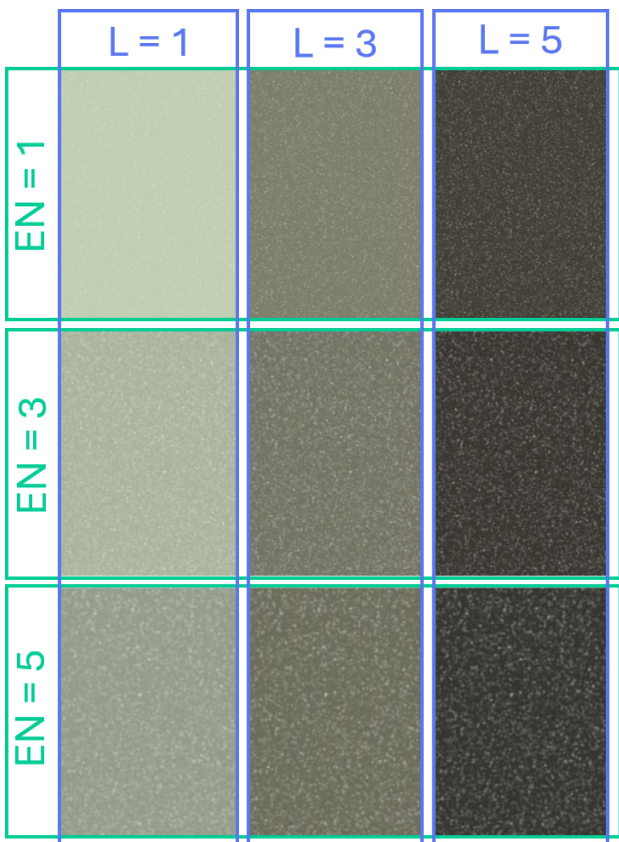


Figure 6. Preliminary rendering example for samples L 1,3,5 / EN 1,3,5 at 45°:0°.

## References

- [1] A. Ferrero, N. Basic, J. Campos, M. Pastuschek, E. Perales, G. Porrovecchio, M. Šmid, A. Schirmacher, J.L. Velázquez, F.M. Martínez-Verdú, "An insight into the present capabilities of national metrology institutes for measuring sparkle", *Metrologia* 57 065029 (2020).
- [2] G. Wyszecki and W. S. Stiles, *Color Science: Concepts and Methods, Quantitative Data and Formulae*. John Wiley & Sons (2000).
- [3] E. Perales, A. Ferrero, J. C. Fernández-Becares, M. Milosevic, J. Campos, K. Huraibat, J. Pérez, "Influencia del tono de los pigmentos de absorción en la percepción de sparkle", *Congreso Nacional del Color*, (2022).
- [4] U. Sperling and P. Schwarz, Device for a goniometric examination of the optical properties of surfaces, US Patent 7,276,719 (2007)
- [5] W.H. Kettler, M. Sormaz and P. Ehbets, Apparatus and method for effect pigment identification, WO/2018/041727 (2017)
- [6] International Commission of Illumination, JTC 12 (D2/D1/D8): THE MEASUREMENT OF SPARKLE AND GRAININESS, (2020), <https://cie.co.at/technicalcommittees/measurement-sparkle-and-graininess>
- [7] Standox, Developed for maximum color accuracy: The Standoblue Color Tools
- [8] A. Ferrero, J. L. Velázquez, E. Perales, J. Campos, F. M. Martínez Verdú, "Definition of a Measurement Scale of Graininess from Reflectance and Visual Measurements", *Opt. Express*, 26 (23), p.30116 (2018)
- [9] A. Ferrero, E. Perales, N. Basic, M. Pastuschek, G. Porrovecchio, A. Schirmacher, J. L. Velázquez, J. Campos, F. M. Martínez-Verdú, M. Šmid, P. Linduska, T. Dauser, and P. Blattner, "Preliminary measurement scales for sparkle and graininess," *Opt. Express* 29, p. 7589-7600 (2021).
- [10] A. Ferrero, J. Campos, A. Rabal, and A. Pons, "A single analytical model for sparkle and graininess patterns in texture of effect coatings," *Opt. Express* 21(22), 26812–26819 (2013).
- [11] E. Kirchner, I. van der Lans, F. Martínez-Verdú, E. Perales. "Improving color reproduction accuracy of a mobile liquid crystal display". *J Opt Soc Am. A*, 34, 101-110 (2017).
- [12] E. Kirchner, I. van der Lans, E. Perales, F. Martínez-Verdú. "Improving color reproduction accuracy of an OLED-based mobile display". *Color Res Appl.*, 43, 34–46 (2018).